EFFECT OF AXIAL DEFORMATION OF COLUMNS ON DYNAMIC BEHAVIOR OF REINFORCED CONCRETE BUILDING FRAMES

by

Koji Yoshimura[I] and Kenji Kikuchi[II]

SUMMARY

The static and dynamic analyses of medium and low-rise reinforced concrete building frames with framed shear walls which are subjected to horizontal and vertical components of ground motions are performed. And the effects of inertias in the vertical directions and the axial deformations of columns on dynamic behavior of the model frames are investigated in the elastic range.

INTRODUCTION

In the current aseismic design method in Japan, the effects of the vertical component of ground motion and the axial deformation of columns in the medium and low-rise building frames are not taken into consideration. In the present paper, the effects of inertias in the vertical direction and axial deformation of columns on dynamic behavior of the reinforced concrete model frames are investigated. In the analysis, forty-five different model frames in which framed shear walls are provided in the various patterns are selected. And for these frames, both static and dynamic response analyses are performed in the elastic range. Special emphasis is placed on dynamic analysis of the six-story reinforced concrete frames with soft and hard stories in case when these frames are subjected to horizontal and vertical components of ground motions. In the recent studies on dynamic analyses in which building structures are subjected to horizontal and vertical simultaneous ground motions, simplified structural models were frequently adopted except for a few studies[1]. In the present study, stiffness of the beams, columns and framed shear walls are evaluated as precise as possible.

METHOD OF ANALYSIS

Model Frames. Three-bay-six-story reinforced concrete plane frames in which framed shear walls are arranged apart in the various patterns were selected as the typical model frames. Fig. 1 shows over-all dimensions and distribution of weights of the model frames used in the analysis. Dead plus live loads at each floor level were lumped at the beam-to-column connections. Fig. 2 shows the details of the framed shear walls provided in the frames. Cross-sectional dimensions of this framed shear walls are the same with those of the illustrative example in 1979 AIJ (Architectural Institute of Japan) Standard for Structural Calculation of Reinforced Concrete Structures. Schematic elevations of the model frames are given in Fig. 3. Cross-sectional dimensions of all columns and beams are respectively the same as those of the boundary frames of the framed shear walls in Fig. 2, except that the depth of footing beams is 1.0 meter.

I Associate Professor, Department of Architecture, Oita University, Japan
II Research Assistant, Department of Architecture, Oita University, Japan

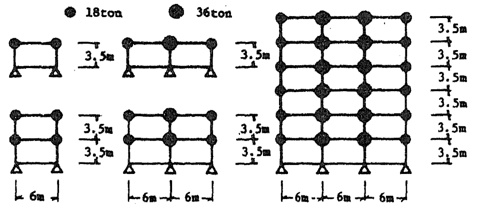

Fig. 1 Distribution of Weights

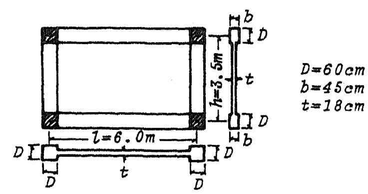

Fig. 2 Framed Shear Wall

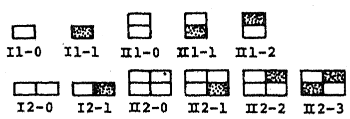

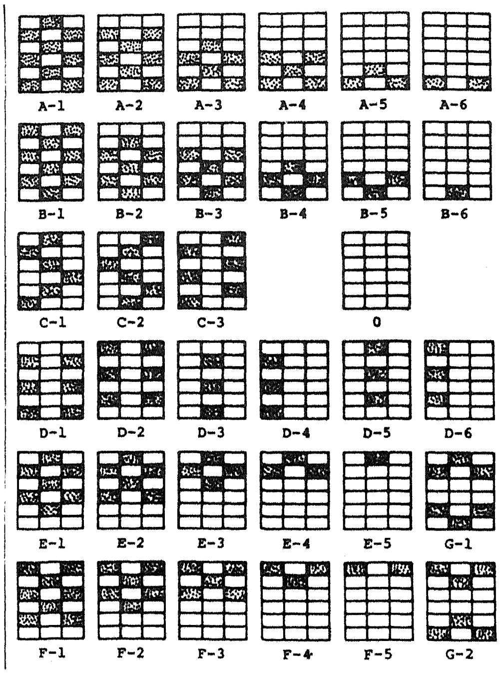

Fig. 3 Arrangement of Shear Walls in Model Frames

Stiffness of Beam, Column and Shear Wall Elements. Stiffness matrices of the beam and column elements were determined by taking into account of the flexural and shear deformations. Because each floor was assumed to act as a rigid horizontal diaphragm in its own plane, beams have no axial deformation. It was assumed, however, that the columns have axial deformation. Presence of rigid zones in the beam-to-column connections was also taken into account. Stiffness matrix determined by using Airy's stress function was used in order to evaluate the rigidity of the framed shear wall. This stiffness matrix proposed by M. Tomii, T. Yamakawa and H. Hiraishi is only applicable to the linear elastic analysis of reinforced concrete structures with framed shear walls arranged apart[2),3)].

Analytical Models. In order to examine the effects of axial deformation of columns and vertical inertias on dynamic behavior of the model frames, four different models were selected according to the directions of nodal displacements and inertias which were taken into consideration. Table 1 shows the schematic drawings of nodal displacements and directions of inertias considered in each model.

Table 1 Nodal Displacements and Inertias

Model	$(D_{HV}I_{HV})$	$(D_{HV}I_H)$	(D_HI_H)	(D_VI_V)
Nodal Displacements	Node, u, v, Column Deformation	u, v	u, v=0	v, u=0
Direction of Inertias	V, H	H	H	V

Symbols "D" or "I" in the table denote the nodal displacement or inertia respectively, and the subscripts "H" or "V" represent that the horizontal or vertical inertias at each node are taken into account. In Model $(D_{HV}I_{HV})$, nodal displacements and inertias in both horizontal and vertical directions are taken into consideration, and therefore this model is the most realistic among the four analytical models. While in Model ($D_{HV}I_H$), the nodal displacements in both horizontal and vertical directions are taken into account but the inertias are considered only in the horizontal direction. In Model (D_HI_H) or Model (D_VI_V), nodal displacements and inertias only in the horizontal or vertical directions are considered respectively. Models ($D_{HV}I_H$) and (D_HI_H) were selected to examine the effect of vertical inertias and axial column deformations on dynamic response of the model frames which are subjected to uni-directional horizontal ground motions, and Model (D_VI_V) was to investigate the dynamic characteristics in the vertical direction. In all models, however, the rotations of nodes are not restricted but rotational inertias are not considered. Stiffness matrices of these four different models have the following relationship. By using the assumptions that the floor slabs are rigid in their own planes and moment acting at each node are equal to zero, static relations between forces acting at each floor level or node and the corresponding displacements can be expressed as

$$\left\{\begin{array}{c}\bar{\mathbf{X}}\\ \hline \mathbf{Z}\end{array}\right\} = \left[\begin{array}{c|c}\mathbf{K}_{\bar{u}\bar{u}} & \mathbf{K}_{\bar{u}v}\\ \hline \mathbf{K}_{v\bar{u}} & \mathbf{K}_{vv}\end{array}\right]\left\{\begin{array}{c}\bar{\mathbf{u}}\\ \hline \mathbf{v}\end{array}\right\} \quad \cdots\cdots\cdots \quad (1)$$

where
$\{\bar{\mathbf{X}}\}$ = horizontal forces acting at the floor levels,
$\{\mathbf{Z}\}$ = vertical forces acting at the nodes,
$\{\bar{\mathbf{u}}\}$ = horizontal displacements of the floors,
$\{\mathbf{v}\}$ = vertical displacements of the nodes,
$[\mathbf{K}_{\bar{u}\bar{u}}]$ = horizontal forces at each floor level caused by a unit horizontal displacement at a particular floor level,
$[\mathbf{K}_{vv}]$ = vertical forces at each node caused by a unit vertical displacement at a particular node,
$[\mathbf{K}_{\bar{u}v}]$ = horizontal forces at each floor level caused by a unit vertical displacement at a particular node and
$[\mathbf{K}_{v\bar{u}}]$ = vertical forces at each node caused by a unit horizontal displacement at a particular floor level.

The stiffness matrix of Model ($D_{HV}I_{HV}$) is given by the matrix in Eq. 1. And the stiffness matrices of Models ($D_{HV}I_H$), (D_HI_H) and (D_VI_V) are respectively represented by the matrices given in Eqs. 2, 3 and 4.

$$\{\bar{\mathbf{X}}\} = [\mathbf{K}_{\bar{u}\bar{u}}]\{\bar{\mathbf{u}}\} \quad \cdots\cdots\cdots \quad (2)$$

$$\{\mathbf{Z}\} = [\mathbf{K}_{vv}]\{\mathbf{v}\} \quad \cdots\cdots\cdots \quad (3)$$

$$\{\bar{\mathbf{X}}\} = ([\mathbf{K}_{\bar{u}\bar{u}}] - [\mathbf{K}_{\bar{u}v}][\mathbf{K}_{vv}]^{-1}[\mathbf{K}_{v\bar{u}}])\{\bar{\mathbf{u}}\} \quad \cdots\cdots\cdots \quad (4)$$

Static Analysis. Static analysis in case when model frames are subjected to lateral forces and gravity loads were performed to obtain the nodal displacements and member forces including axial forces in the columns. Analytical results obtained were compared with those from dynamic analysis. Two different lateral seismic coefficient distributions were used in the static analysis; one is a nearly rectangular distribution which is specified in the current Japanese Building Standard Law (JBS) and the other is a triangular one specified in the Uniform Building Code (UBC) in USA. The values of seismic coefficient, k_i, used in the analysis are shown in Fig. 4. The triangular distribution was determined so that its

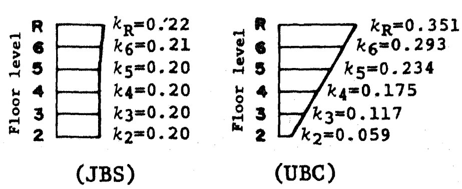

Fig. 4 Lateral Seismic Coefficients

base shear coefficient has the same value with the rectangular one. Axial forces in the columns in case when those frames are subjected to dead plus live loads were determined by using the current practical method in Japan.

Dynamic Analysis. When a model frame is subjected to both horizontal and vertical components of ground acceleration, the equation of motion becomes

$$\left[\begin{array}{c|c} \bar{m} & 0 \\ \hline 0 & m \end{array}\right]\left\{\begin{array}{c} \ddot{\bar{u}} \\ \hline \ddot{v} \end{array}\right\} + \left[\begin{array}{c|c} C_{\bar{u}\bar{u}} & C_{\bar{u}v} \\ \hline C_{v\bar{u}} & C_{vv} \end{array}\right]\left\{\begin{array}{c} \dot{\bar{u}} \\ \hline \dot{v} \end{array}\right\} + \left[\begin{array}{c|c} K_{\bar{u}\bar{u}} & K_{\bar{u}v} \\ \hline K_{v\bar{u}} & K_{vv} \end{array}\right]\left\{\begin{array}{c} \bar{u} \\ \hline v \end{array}\right\} = - \left[\begin{array}{c|c} \bar{m} & 0 \\ \hline 0 & m \end{array}\right]\left\{\begin{array}{c} \ddot{X}_G \\ \hline \ddot{Z}_G \end{array}\right\} \quad \ldots . \ (5)$$

where $[\bar{m}]$, $[m]$ = mass matrices, $[C]$ = damping matrices and $\{\ddot{X}_G\}$, $\{\ddot{Z}_G\}$ = horizontal and vertical ground accelerations. The computations of dynamic response to ground acceleration were performed by using the normal mode method and the equation of motion was solved by using a step-by-step integration method. The modes of vibration which are higher than 10^{th} mode were ignored. The time interval of a given earthquake accelerogram is 0.002 seconds. Damping ratios were assumed to be 5 percent of the critical damping in each mode of vibration. In the dynamic analysis, digitized data of both horizontal and vertical components of three different strong motion earthquake records shown in Table 2 were used. Table 3 shows the components of input ground motions and the peak accelerations adopted in the analysis.

Table 2 Earthquake Records

Earthquake	EL CENTRO 1940	TAFT 1952	OITA 1975
Horizontal Component	N-S (341.7)	S69E (175.6)	E-W (70.6)
Vertical Component	VERT. (206.3)	VERT. (102.9)	VERT. (29.3)
Duration	10 Sec.	15 Sec.	10 Sec.

Note : Recorded Peak Acceleration (Gals) in Parenthesis

Table 3 Input Peak Acceleration (Gals)

	Horizontal Component	Vertical Component
Horizontal Direction	200	0
Vertical Direction	0	100
Horizontal and Vertical Direction	200	¶

$$¶ = \frac{\text{Recorded Peak Acceleration of Vertical Component}}{\text{Recorded Peak Acceleration of Horizontal Component}} \times 200$$

RESULTS OF ANALYSIS AND DISCUSSIONS

Fundamental Periods. Eigen values of all model frames were determined by using the Q-R method. The relations between fundamental periods of Models ($D_{HV}I_{HV}$) and ($D_V I_V$), which are designated by ${}_HT_1$ and ${}_VT_1$ respectively, are given in Fig. 5. All of the first modes of vibration in Model ($D_{HV}I_{HV}$) are horizontal modes. The figure shows that the values of ${}_HT_1$ in six-story model frames are widely scattered between 0.19 and 0.95 seconds, while those of ${}_VT_1$ are within the range between 0.079 and 0.099 seconds. As a result, ${}_VT_1$ are not remarkably affected by the manner of arrangement of shear walls. Similar tendency can be observed in the low-rise model frames. Open circles in Fig. 6 represent the comparison of fundamental periods of horizontal

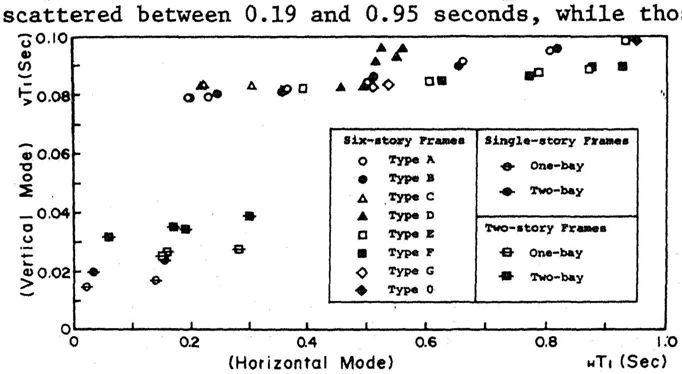

Fig. 5 Fundamental Period of Vibration

modes between two Models, ($D_{HV}I_{HV}$) and ($D_{HV}I_H$). This figure shows that most of the fundamental periods in Model ($D_{HV}I_H$) have a good agreement with those in Model ($D_{HV}I_H$). On the contrary, fundamental periods of vibration in Model (D_HI_H) are compared with those in Model ($D_{HV}I_{HV}$) by using solid circles in Fig. 6. It is noted that in case when axial deformations of columns are ignored, fundamental periods of frames of Type D in Fig. 2 or frames, in which framed shear walls are provided all over the stories (Types A-1, B-1 and C), are considerably shortly evaluated.

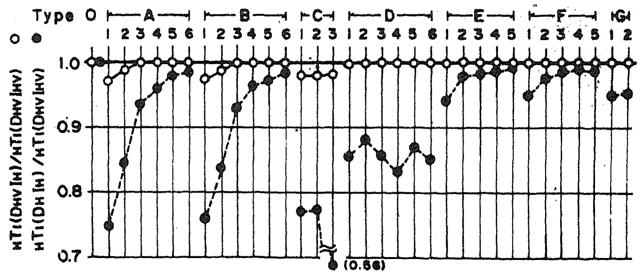

Fig. 6 Fundamental Periods of Horizontal Modes

Approximate Solution of Fundamental Period of Vertical Modes. In determining the fundamental period of vibration approximately, Geiger's equation is frequently used. This equation is practically applicable to determine the fundamental period of the horizontal mode, if horizontal stiffness of the whole structure can be evaluated acculately[4]. In the present section, validity of Geiger's equation to determine the fundamental period of vertical modes is investigated. In this case, a simple model in which rigid floor slabs can be allowed to move only in the vertical direction was adopted (refer to Fig. 7). Vertical stiffness of the framed shear walls in the adopted model, however, was determined in accordance with the exact solution proposed by M. Tomii et al. as shown in Fig. 8. Fig. 9 shows the comparison between fundamental period of vertical modes determined from the exact solutions, ${}_VT_1$, and approximate ones, ${}_VT_1'$, determined from Geiger's equation. It is understood from the figure that the fundamental period of vertical modes can be evaluated by the approximate method within the errors less than ± 8 percent, if the value of constant in Geiger's equation is choosen adequately.

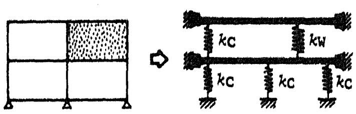

Fig. 7 Simplified Vertical Springs

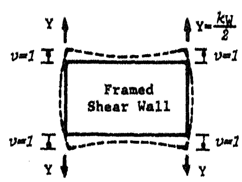

Fig. 8 k_W in Shear Wall

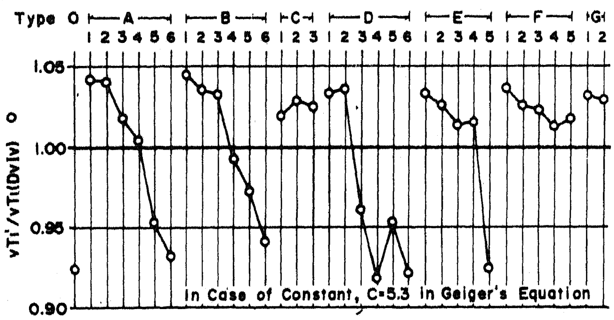

Fig. 9 Approximate Solutions of Fundamental Period in Vertical Modes

Maximum Story Shears and Story Drifts. Fig. 10(a) shows typical examples of the envelops of maximum story shear coefficients caused by El Centro 1940 ground motions. Note that the envelops of maximum story shear coefficients in model ($D_{HV}I_{HV}$) caused by the horizontal and vertical simultaneous ground motions are nearly coincide with those caused by the uni-directional horizontal ground motions. In addition, in case when the model frames are subjected only to the horizontal component of ground motion, story shear coefficients of Model ($D_{HV}I_H$) almost agree with those of Models ($D_{HV}I_{HV}$) and (D_HI_H). And also it can be seen from the figure that values of story shear coefficients of Model ($D_{HV}I_{HV}$) caused by the vertical ground motion are quite small and are 0.05 at the most. Fig. 10(b) shows typical examples of maximum story drifts in Model ($D_{HV}I_{HV}$). Again, the maximum story drifts caused by the simultaneous ground motions are almost the same as those caused by the horizontal ground motion. In addition, those values are nearly equal to those in Model ($D_{HV}I_H$) caused by the same horizontal ground motion. Similar tendency was observed when Taft 1952 ground motions was used. As the results, the vertical component of ground motions and inertias in the vertical direction have not large effects on maximum story shears and story drifts of the model frames.

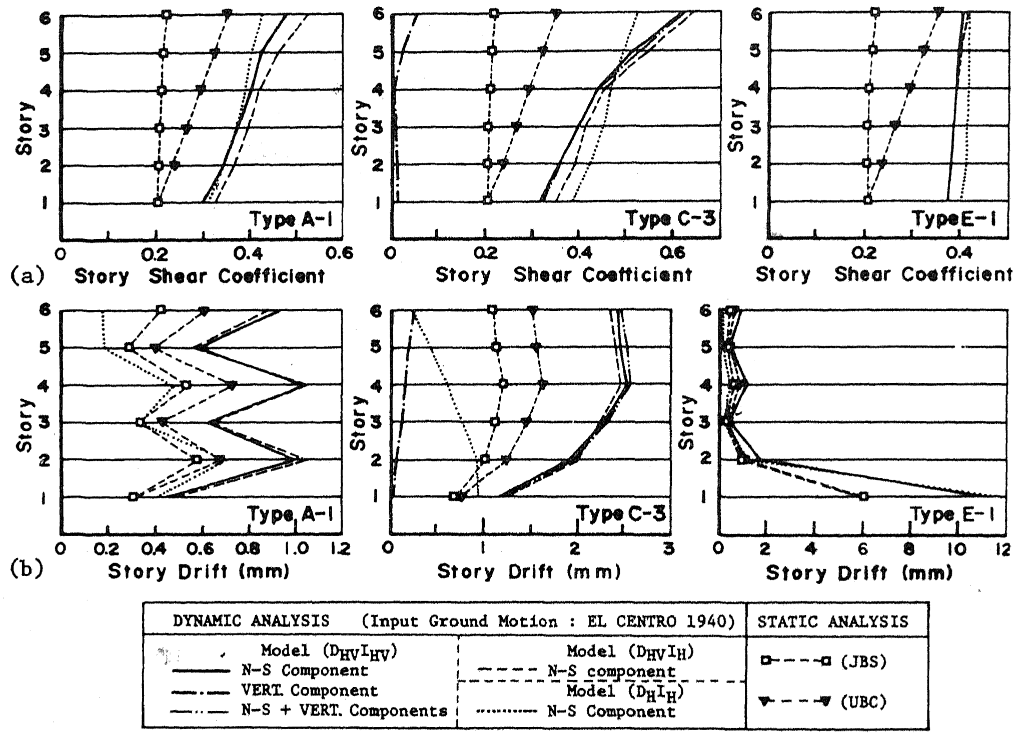

Fig. 10 Maximum Story Shear Coefficients and Maximum Story Drifts

Maximum Compressive Stresses in First Story Columns. For the fourteen model frames in which framed shear walls are not provided in the lower stories, maximum values of axial compressive stresses in the first story columns were examined by using Model ($D_{HV}I_{HV}$). Fig. 11 shows the results calculated from dividing the values of (${}_DN + N_L$) by (${}_SN + N_L$), in which ${}_DN$ and ${}_SN$ are the axial compressive stresses caused by dynamic motions and JBS static lateral forces respectively, and N_L is the axial stresses caused by static dead plus live loads. It can be seen from the figure that the values of (${}_DN + N_L$) are considerably greater than (${}_SN + N_L$). Moreover, large axial stresses are induced in some interior columns in case when model frames are subjected to vertical and horizontal simultaneous ground motions. In Fig. 12, maximum axial stresses

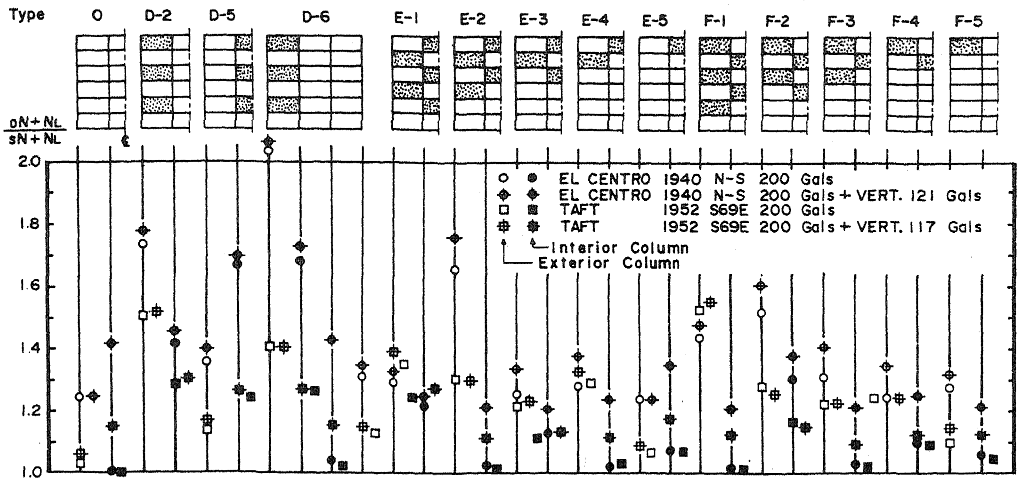

Fig. 11 Maximum Axial Stresses in First Story Columns Caused by Uni-directional or Simultaneous Ground Motions

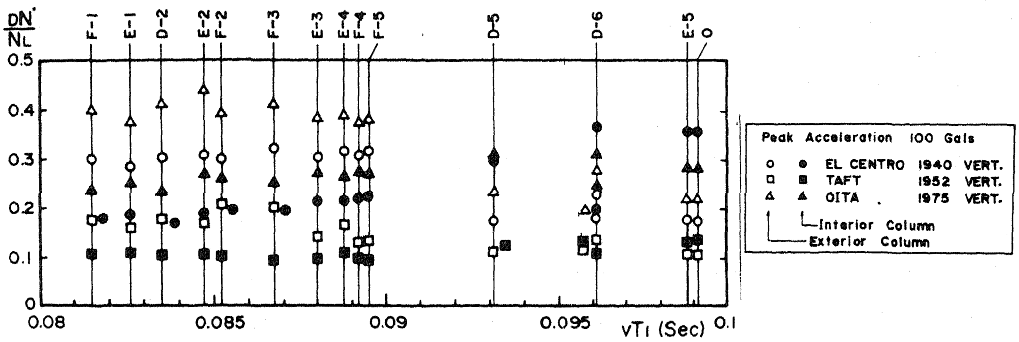

Fig. 12 Maximum Axial Stresses in First Story Columns Caused by Vertical Ground Motions

in the first story columns caused by a vertical ground motion, $_DN'$, are compared with the values of N_L. The abscissa of the figure represents the fundamental period of vertical modes, $_VT_1$. This figure shows that the vertical ground motions with peak acceleration of 100 Gals have a large effect on axial stresses in the first story columns and the values of $_DN'$ are about 10 to 40 percent larger than those of N_L. As a result, the effect of vertical component of ground motion on axial stresses in the first story columns could not be ignored.

Relation between Maximum Base Shears and Axial Stresses in Columns. Fig. 13 shows the relation between maximum base shear coefficients, $_DC_1$, and maximum axial compressive stresses in the first story columns, $_DN$, when Model ($D_{HV}I_{HV}$) is subjected to N-S component of El Centro 1940 with 200 Gals peak acceleration. These values are given by dimensionless forms using the values of $_SC_1$ and $_SN$ respectively, where $_SC_1$ and $_SN$ are the corresponding values caused by static lateral forces. It can be seen from the figure that the values of $_DN/_SN$ are nearly proportional to $_DC_1/_SC_1$. This fact shows that the value of $_DN$ can be approximately estimated from the value of $_DC_1$. It is noteworthy that in case when the values of $_SN$ are determined from the static lateral forces specified in JBS, all of the values of $_DN/_SN$ fall upper than the line along the level 45 degrees. On the contrary, if the values of $_SN$ are determined from UBC, most of the values of $_DN/_SN$ fall lower than the same line. As the result, in case when the value of $_DN$ is estimated from the value of $_DC_1$, the value of $_DN$ determined by UBC would become more conservative than by JBS.

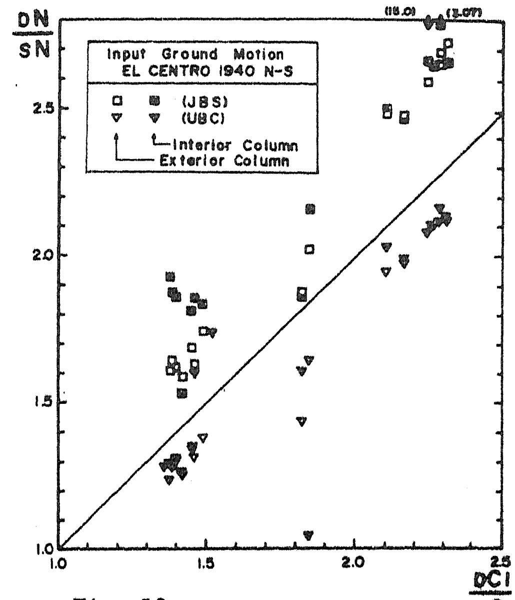

Fig. 13
Relation between Maximum Base Shears and Axial Stresses in First Story Columns

CONCLUDING REMARKS

(1). The effect of the manner of arrangement of framed shear walls on fundamental period of vertical modes in reinforced concrete frames with framed shear walls can be neglected.
(2). Fundamental period of vertical modes can be approximately evaluated by Geiger's equation.
(3). If the axial deformations of columns are not taken into analysis, fundamental periods of horizontal modes in some frames are considerably shortly evaluated.
(4). The effect of vertical ground motions on maximum story shears and maximum story drifts can be neglected.
(5). The effect of vertical ground motions on maximum axial stresses in the first story columns cannot be disregarded. It is worthy of note that considerably large axial stresses are induced in some interior columns in case when model frames are subjected to vertical and horizontal ground motions.
(6). Vertical inertias of nodes caused by uni-directional horizontal ground motions have not a large effect on dynamic responses of the model frames.

REFERENCES

(1). Anderson J. C. and Bertero V. V., "Effects of Gravity Loads and Vertical Ground Acceleration on the Seismic Response of Multistory Frames," Report No. EERC 73-23, Earthquake Engineering Research Center, University of California, Sept., 1973, 175-184 pp.
(2). Tomii M. and Hiraishi H., "Elastic Analysis of Framed Shear Walls by Considering Shearing Deformation of the Beams and Columns of Their Boundary Frames," Parts I to III, Trans. of the Architectural Institute of Japan, Nos. 273 to 275, Nov. and Dec., 1978, and Jan., 1979.
(3). Tomii M. and Yamakawa T., "Relations between Nodal External Forces and the Nodal Displacements on the Boundary Frames of Rectangular Elastic Framed Shear Walls," Parts I to V, Trans. of the Architectural Institute of Japan, Nos. 237 to 241, Nov. and Dec., 1975, and Jan., Feb. and Mar., 1976.
(4). Yoshimura K. and Inoue M., "Dynamic Analysis of Reinforced Concrete Frames with Framed Shear Walls," Preprints of 6WCEE, New Delhi, Jan., 1977.